Divergence Factor in Ray Model and Its Application to Light Scattering by a Large Nonspherical Dielectric Particle

Ce Zhang, Claude Rozé, and Kuan Fang Ren

***Abstract*—This letter focuses on the description of the divergence factor of a wave in terms of differential geometry, called vectorial complex ray model (VCRM), and its application in the scattering of a large nonspherical dielectric particle. The VCRM permits to calculate the amplitude and the phase of electric field rigorously in terms of ray model, but it fails to predict correctly the field near caustics (in rainbow angles). This problem is solved by combining the field calculated with VCRM and the physical optics. This hybrid method is then applied, as example, to the scattering of an infinite cylinder and an ellipsoid. The comparison with the rigorous Debye theory shows that our method can predict very precisely the scattered field in all directions including near the rainbow angles. The hybrid method removes the two approximations in Airy theory, so the results are much better. Because of its flexibility, this method can be applied directly to the scattering of a large nonspherical object of smooth surface.**

***Index Terms*—Caustics, divergence factor, large nonspherical particle, physical optics, scattering, vectorial complex ray model (VCRM).**

I. Introduction

RESEARCH on electromagnetic wave scattering by particles (or objects) is important to both science and technology [1], [2], [3], [4]. According to the scattered field, the parameters of the objects/particles, such as size, shape, and temperature, can be deduced. So, accurate and efficient methods for scattering are crucial for the applications in many fields. However, the computation of the scattering field by large nonspherical objects is still a challenge.

The methods to deal with the scattering can be briefly divided into three kinds. The first is the rigorous theories, such as Mie theory and Debye theory [3], [4], [5]. Theoretically, these methods can be applied to the objects of any size, but they are limited to the object of very simple shape like infinite circular cylinders and spheres. There exists also solution for the spheroid [6], but the size is limited [7]. The second kind concerns the numerical methods such as finite-difference time domain [8], discrete dipole approximation [9], method of moment [10], multilevel fast multipole algorithm (MLFMA) [11], [12], etc. The shape of the objects is no longer limited, but they are resource consuming. The third kind is the approximation models, such as the physical optics approximation, the geometrical diffraction theory, the high-frequency method, or the ray models. Usually they need less computation resources, but their precision is limited and each method has its specific application domain.

The combination of the geometrical optics (GO) and the physical optics (PO) is a good compromise. This combined method GO+PO (also called shooting and bouncing rays) has been applied to the scattering by cavities, airplane, and aircraft carrier [13], [14], [15], [16]. But its accuracy is still not satisfactory and there is no general solution to incorporate the divergence factor in the scattering procedure.

In recent years, the vectorial complex ray model (VCRM) has been developed [17], [18], in which the wavefront curvature (WFC) is considered as an intrinsic property of the rays. Thus, the amplitude and the phase of all the individual rays can be calculated easily. Its results for the scattering of an ellipsoidal particle are in good agreement with those of MLFMA and experimental measurement [11], [19], [20]. However, it still fails near the caustics (in rainbow angles for example). In order to remedy this problem, we propose to combine the VCRM and PO to calculate the scattering field near the caustics. The contributions of divergence factor to ray model and the hybrid method VCRM+PO will be described and examined in this letter.

The rest of this letter is organized as follows. To simplify the presentation, we begin in Section II by the definition of the divergence factor and the recall of essential aspects of GO for the scattering of an infinite circular cylinder in order to introduce the terminology and to evaluate the precision of GO by comparison with rigorous Mie theory. In Section III, the VCRM and the hybrid method VCRM+PO are presented. The numerical results are given and discussed in Section IV. Finally, Section V concludes this letter.

II. Definition of the Divergence Factor and GO for Scattering of a Circular Cylinder

In the VCRM, waves are described by rays. Each ray represents the properties of the wave along the ray. When a wave propagates in a homogeneous medium, its intensity varies according to the divergence or convergence of the wave. We call the ratio of the intensities at two points along the same ray due to the divergence of WFC and the *divergence factor* $\mathfrak{D}$.

Manuscript received 2 September 2023; accepted 29 September 2023. Date of publication 5 October 2023; date of current version 5 January 2024. This work was supported in part by the National Key Research and Development Program of China under Grant 2018YFA0701900 and Grant 2018YFA0701904, and in part by the China Scholarship Council under Grant 201906960009. *(Corresponding author: Kuan Fang Ren.)*

Ce Zhang is with the State Key Laboratory of Millimeter Waves, Southeast University, Nanjing 210096, China (e-mail: cezhang@seu.edu.cn).

Claude Rozé is with the CORIA-UMR 6614, CNRS, Université et INSA de Rouen, 76801 Saint-Etienne du Rouvray, France (e-mail: claude.roze@coria.fr).

Kuan Fang Ren is with the CORIA-UMR 6614, CNRS, Université et INSA de Rouen, 76801 Saint-Etienne du Rouvray, France, and also with the School of Physics, Xidian University, Xi'an 710071, China (e-mail: fang.ren@coria.fr).

Digital Object Identifier 10.1109/LAWP.2023.3322225

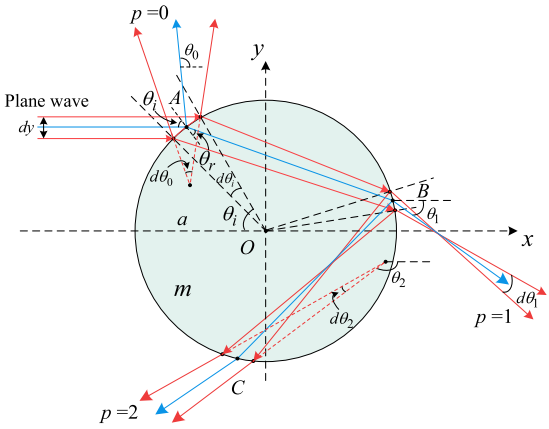

Fig. 1. Ray model in scattering of an infinite circular cylinder.

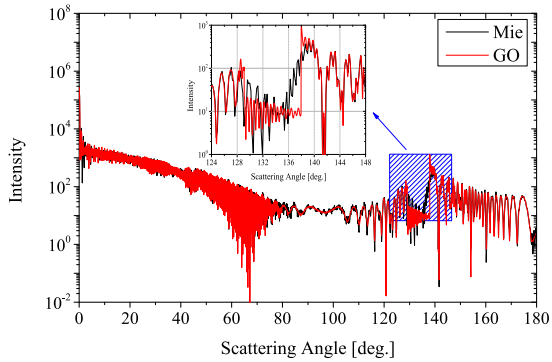

Fig. 2. Comparison of the scattering diagrams of an infinite circular cylinder ($\lambda = 0.6328\,\mu$m, $a = 50\,\mu$m, $m = 1.333$) calculated by the Mie theory and the GO for the perpendicular polarization.

If a ray interacts with a dioptric surface, the intensities of the reflected and refracted rays are affected by two factor. The first, called Fresnel factor ε, is due to the reflection or refraction on the surface and can be calculated by the Fresnel formulas. The second is the divergence factor $\mathfrak{D}$, which is the ratio of the intensity on a point of reflected or refracted ray over that at the incident point as if $\varepsilon = 1$. These definitions can be extended to the interaction of a ray with a particle, i.e., the intensity of the emergent ray I_e is related to that of the incident ray I_i by

$$I_e = \varepsilon \mathfrak{D} I_i \tag{1}$$

where ε and $\mathfrak{D}$ are dimensionless. In general, $\mathfrak{D}$ is affected by the two curvatures of the wavefront surface in 3-D. To ease the discussion, we note in the following by D the divergence factor due to one curvature of the wavefront in a plane.

Consider now a simple 2-D scattering problem, i.e., a circular cylinder of radius a and refractive index m illuminated by a plane wave at normal incidence. In GO, the incident wave is described by bundles of parallel rays (see Fig. 1). The directions of the reflected and refracted rays on the particle surface are governed by Snell's law. Due to the circular symmetry of the cylinder, the deviation angles θ_p of the rays are determined by the incident angle θ_i, the refractive index m and the order p of the emergent ray (convention of [3], see Fig. 1). The relation between the intensities in far field of the emergent ray I_p of order p and the incident ray I_i is established [3] by the energy balance as

$$I_p(r, \theta_p) r |d\theta_p| = \varepsilon I_i |dy| = \varepsilon I_i a \cos\theta_i |d\theta_i|$$

where r is the distance from the particle center O to the observation point. According to (1), we identify that the 2-D divergence factor $D_{2D} = \frac{a\cos\theta_i}{r} |\frac{d\theta_i}{d\theta_p}|$. The derivative $\frac{d\theta_i}{d\theta_p}$ for a circular cylinder can be found analytically [3] and the divergence factor is deduced to be $D_{2D} = \frac{a}{r} D$ with [22]

$$D = \frac{m \cos\theta_i \cos\theta_r}{2\,(p\cos\theta_i - m\cos\theta_r)} \tag{2}$$

where θ_r is the refraction angle of the ray on the particle surface. The Fresnel factor ε is given as follows:

$$\varepsilon = \begin{cases} r_X^2, & p = 0 \\ (1 - r_X^2)^2 (-r_X)^{2(p-1)}, & p \neq 0 \end{cases} \tag{3}$$

with r_X the Fresnel reflection coefficient in polarization X ($X = \perp$ or $\parallel$ for perpendicular or parallel polarization). The complex amplitude of the scattered wave in far field, by omitting the cylindrical factor $1/\sqrt{k_0 r}$, is [21]

$$E_{X,p}(\theta_p) = E_0 \sqrt{\frac{\pi}{2} k_0 a \varepsilon D} e^{i\Phi_T} \tag{4}$$

where E_0 is the amplitude of the incident plane wave, and k_0 the wave number in the surrounding medium. The total phase of the ray Φ_T is composed of four parts

$$\Phi_T = \Phi_i + \Phi_P + \Phi_F + \Phi_f \tag{5}$$

Φ_i is the phase of the incident wave, Φ_P is the phase due to the optical path, Φ_F is the phase caused by the Fresnel coefficient, and Φ_f is the phase shift due to the focal lines (type a in [3]).

The total scattering field in a given direction is then the summation of the complex amplitudes of all the emergent rays in that direction and of the forward diffraction. The scattering diagrams calculated by the above described GO and the Mie theory are compared in Fig. 2. In the calculation, the number of the incident rays and the scattering angle divisions are both 7000 and the maximum order is $p = 7$. We find that the scattering diagrams of the two methods are in good agreement except in the rainbow region between 128° and 139°. We have also compared the scattering diagram of a spherical particle calculated by the two methods (not given here) and found the similar results. We can therefore conclude that by taking into account correctly the divergence factor and all the phases of the rays, the GO can predict precisely the scattering diagrams of a large particle [22] except in certain regions.

However, two problems remain to be solved: the correction of the scattered field near the rainbow angles and the scattering of a nonspherical particle. We will show that the VCRM [18], [20], [23] permits to solve the two problems at the same time.

III. VCRM and VCRM+PO for the Scattering of a Large Dielectric Particle

In the VCRM, the WFC is described by a 2×2 matrix and the relation between the WFCs of the reflected and the refracted waves with those of the incident wave and the particle surface is given by the wavefront equation [18]. The amplitude and the phase of a wave at any point can be evaluated step by step in the VCRM.

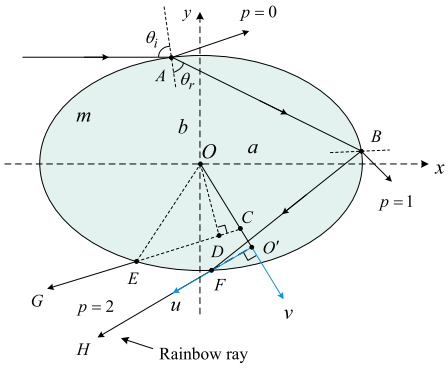

Fig. 3. Ray model near the rainbow angle of an ellipsoidal particle.

TABLE I
WFCR (μM) OF RAYS NEAR RAINBOW ANGLE

Angle(°)	$R'_{2,1}$	$R_{2,2}$	$R'_{2,2}$	$R_{2,3}$	$R^e_{2,3}$
...	...	...	...	...	...
150.5438	40.857	-26.335	46.385	-20.807	-1.785
150.3154	41.048	-26.186	46.937	-20.297	-1.754
...	...	...	...	...	...
137.9222	76.119	-0.174	-0.176	-76.469	5517.2
137.9220	76.246	-0.079	-0.079	-76.405	12237.7
137.9219	76.373	0.016	0.016	-76.341	-60052.0
137.9220	76.500	0.111	0.111	-76.278	-8782.1
...	...	...	...	...	...
150.3112	149.639	57.875	16.429	-75.335	-97.232
150.3373	149.730	57.950	16.437	-75.343	-97.230
...	...	...	...	...	...

A. Principle of VCRM

To ease the explanation, we consider the scattering in the plane xy of an ellipsoid illuminated by a plane wave along x-axis (see Fig. 3). In this case, the WFCs perpendicular and parallel to this plane are independent and the wavefront equation [17], [18] is simplified to two scalar equations

$$\frac{k'}{R'_1} = \frac{k}{R_1} + \frac{k'\cos\theta' - k\cos\theta}{\rho_1} \tag{6}$$

$$\frac{k'\cos^2\theta'}{R'_2} = \frac{k\cos^2\theta}{R_2} + \frac{k'\cos\theta' - k\cos\theta}{\rho_2} \tag{7}$$

where k and k' are, respectively, the wave numbers of the incident and refracted/reflected rays. The index $\nu = 1, 2$ stands, respectively, for the WFCs in the direction perpendicular and parallel to the incident plane. ρ_ν being the curvature radii of the particle surface at the interaction point, and R_ν and R'_ν are the wavefront curvature radii (WFCR) before and after interaction. The relation between the WFCR at two successive interaction points and their distance d_q is $R_{\nu,q+1} = R'_{\nu,q} - d_q$, where q being the interaction number.

The intensity I_{q+1} of the ray incident on the $(q+1)$th interaction point being related to the intensity I'_q of the ray emergent from qth interaction point by $I_{q+1} = I'_q \frac{R'_1 R'_2}{R_1 R_2}$, we deduce from (1) that the divergence factor between the point on the pth order emergent ray at distance d and the first incident point is given by $\mathfrak{D}_p = D_{1,p} D_{2,p}$ [18] with

$$D_{\nu,p} = \left| \frac{R'_{\nu,1}}{R_{\nu,2}} \cdot \frac{R'_{\nu,2}}{R_{\nu,3}} \cdots \frac{R'_{\nu,p}}{R_{\nu,p+1}} \cdot \frac{R^e_{\nu,p+1}}{(R^e_{\nu,p+1} - d)} \right| \tag{8}$$

where d is the distance from the emergent point to the observation point P, and $R^e_{\nu,p+1}$ is the WFCR of the emergent ray. The complex amplitude of the wave at P is calculated by

$$E^{ell}_{X,p}(P) = E_0 \sqrt{\varepsilon D_{1,p} D_{2,p}} \exp\left(i\Phi_T\right). \tag{9}$$

For a nonspherical particle, the Fresnel factor ε must be calculated step by step [20] since the incident angle is no longer constant. The formula of the total phase Φ_T of an emergent ray is the same as (5), but all the four phases must also be calculated step by step.

In the special case of scattering by an infinite cylinder, one of the curvature radii of the particle surface is infinite, $\rho_1 = \infty$, only (7) is necessary. The complex amplitude is given by

$$E^{cyl}_{X,p}(P) = E_0 \sqrt{\frac{\pi}{2} \varepsilon D_{2,p}} \exp\left(i\Phi_T\right). \tag{10}$$

In far field, d tends to r in (8). The complex amplitude of a ray is obtained by (9) or (10) by setting $d = r$. The total scattered field in a given direction is the summation of all the rays emergent in that direction. In the calculation, the spherical wave factor $1/k_0 r$ and the cylindrical wave factor $1/\sqrt{k_0 r}$ are often omitted. In the cases of light scattering by an infinite circular cylinder and a sphere, all formulas of GO can be deduced from VCRM [22].

B. Wavefront Character of Rays in Caustics

In caustics, such as the GO rainbow angles θ_R, the deviation of the rays reach extreme. The WFCR tends to infinity and changes the sign. In the Airy theory [24], the phase of the wave around θ_R is approximated by a cubic function and the amplitude is supposed to be constant. This procedure permits to correct the scattered field predicted by the GO, but the two approximations are only valid in the vicinity of θ_R. The VCRM can calculate the phase of each ray rigorously in terms of ray model. As an example, Table I compiles the values of WFCR of the rays near $\theta_R = 137.9219°$ for the same particle as in Fig. 2. $R'_{2,1}$ is the WFCR of the refracted ray at the first interaction point (A in Fig. 1). The values are all positive representing that the waves are convergent. The WFCRs of the reflected wave $R'_{2,2}$ at point B are positive except at angles near θ_R. When they arrive at point C, $R_{2,3}$ become all negative. The WFCR of the emergent rays $R^e_{2,3}$ change the sign in the rainbow angle θ_R. In the region where the angle is bigger than θ_R, there are two rays folded in far field so they interfere to generate the supernumerary bows (see Section IV).

C. Hybrid Method VCRM+PO for the Scattering of a Large Dielectric Particle in the Rainbow Region

In order to remedy the field around θ_R, we adopt the method of the Airy theory, i.e., calculate first the complex amplitude on a virtual line by using the VCRM and then apply the PO to obtain the scattered intensity in far field. We choose the orthogonal coordinates $(O' : u, v)$, as shown in Fig. 3, with u-axis along the rainbow ray and v-axis perpendicular to u-axis and passing by the particle center O. The complex amplitude on the virtual line v of any emergent ray (EG in Fig. 3) is calculated with (9). The

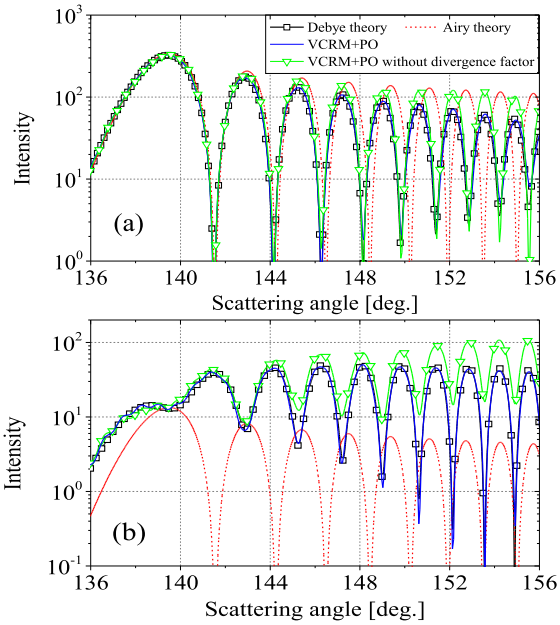

Fig. 4. Scattering diagrams near rainbow angle $p = 2$ with the same parameters as Fig. 2. (a) Perpendicular polarization. (b) Parallel polarization.

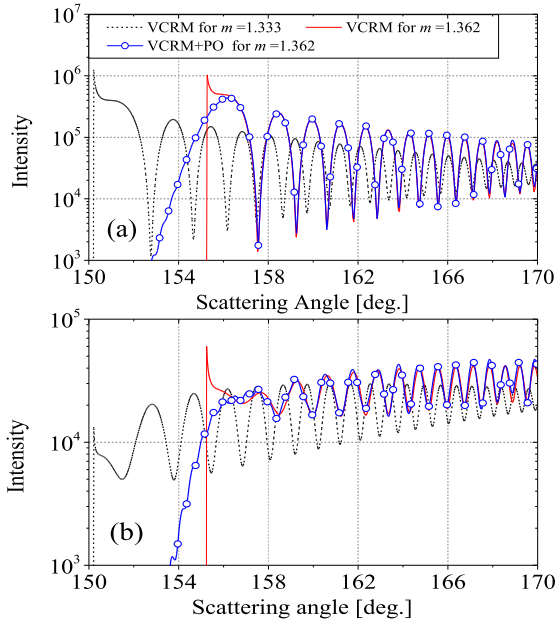

Fig. 5. Scattering diagrams of a spheroid ($a = c = 100\,\mu$m and $b = 90\,\mu$m) on the symmetric plane for $p = 2$. (a) Perpendicular polarization. (b) Parallel polarization.

distance d in (8) is $d = -|\overline{CE}|$. The scattered field is calculated according to the Huygens–Fresnel principle as [4]

$$E_s^{ell}(\theta) = E_0 \frac{k_0}{\sqrt{2\pi}} \int_{v_0}^{v_1} \sqrt{\varepsilon D_{1,p} D_{2,p}} \exp\left[i\Phi(v)\right] dv \quad (11)$$

where the lower and upper boundaries v_0, v_1 are determined by the effective rays on the virtual line v. $\Phi(v) = \Phi_T(v) - kv\sin(\theta - \theta_R)$ with $\Phi_T(v)$ the phase of the emergent ray on the virtual line. For an infinite cylinder, (11) is reduced to

$$E_s^{cyl}(\theta) = E_0 \frac{k_0}{2} \int_{v_0}^{v_1} \sqrt{\varepsilon D_{2,p}} \exp\left[i\Phi(v)\right] dv. \quad (12)$$

IV. Numerical Results and Discussion

The scattering diagrams in the primary rainbow region calculated by the method described in the previous sections are shown in Fig. 4 for an infinite circular cylinder and in Fig. 5 for a spheroidal particle (i.e., an ellipsoid with $a = c$).

Fig. 4 illustrates that for both the perpendicular and parallel polarizations, the results of the VCRM+PO agree very well with Debye theory. The results of VCRM+PO without divergence factor are also given to show its importance on the amplitude evaluation. The Airy theory and the Debye theory agree near θ_R for the perpendicular polarization but the discrepancy becomes obvious when the scattering angle deviates far from θ_R. This is due to the two approximations in Airy theory indicated above and discussed in details for a sphere in [25]. In the parallel polarization, the results of the Airy theory are wrong because in this case the amplitude and the phase vary fast, and the two approximations in Airy theory are not valid at all (see [25], [26], and [27] for sphere).

The scattering diagrams of the spheroidal particle in a symmetric plane (see Fig. 3) calculated by the VCRM and the hybrid method are shown in Fig. 5. We note first that the rainbow angles depend on the refractive index m and the shape of the particle. θ_R for $m = 1.333$ is $137.9°$ for a sphere and $150.2°$ for the spheroid, but $155.2°$ when the refractive index of the spheroid is $m = 1.362$.

We have no rigorous solutions to compare for such large particle. However, we have shown [19], [20] that the results of VCRM are in good agreement with experimental measurements except in the vicinity of GO rainbow angles, i.e., around $155.2°$ for $m = 1.362$ (red curves in Fig. 5). The hybrid method VCRM+PO has been just developed to remedy this problem (see Fig. 4). The same method has been applied to the spheroidal particle, and the results are shown with blue curves in Fig. 5. We note that the profiles of the corresponding curves are similar to those in Fig. 4, but the intensity varies more rapidly because the particle size is bigger and the variation amplitude is less important because of the nonspherity.

The number of incident rays and the divisions of the scattering angles are both 7000 for the calculation of the curves in Figs. 4 and 5. The total computation time of each curves is about 0.5 s on a laptop with Intel Core i7-8750H.

V. Conclusion

The VCRM provides an elegant and simple approach to count the divergence factor and the hybrid method VCRM+PO permits to remedy the problem of ray model in the caustics. The effect of the divergence factor in the scattering of nonspherical particle has been examined and the VCRM+PO is applied to the scattering of a cylinder and a spheroidal particle. The extension of this method to 3-D scattering is under study.

References

[1] J. A. Stratton, *Electromagnetic Theory*. New Jersey, NJ, USA: Wiley, 2007.
[2] A. Ishimaru, *Electromagnetic Wave Propagation, Radiation, and Scattering: From Fundamentals to Applications*. New Jersey, NJ, USA: Wiley, 2017.

[3] H. C. v. d. Hulst, *Light Scattering by Small Particles*. New York, NY, USA: Courier, 1981.
[4] M. Born and E. Wolf, *Principles of Optics: Electromagnetic Theory of Propagation, Interference and Diffraction of Light*. New York, NY, USA: Cambridge Univ. Press, 2013.
[5] E. A. Hovenac and J. A. Lock, "Assessing the contributions of surface waves and complex rays to far-field Mie scattering by use of the Debye series," *J. Opt. Soc. Amer. A*, vol. 9, no. 5, pp. 781–795, 1992.
[6] S. Asano and G. Yamamoto, "Light scattering by a spheroidal particle," *Appl. Opt.*, vol. 14, pp. 29–49, 1975.
[7] F. Xu, J. A. Lock, and G. Gouesbet, "Debye series for light scattering by a nonspherical particle," *Phys. Lett. A*, vol. 81, no. 4, 2010, Art. no. 043824.
[8] P. Yang and K. N. Liou, "Finite-difference time domain method for light scattering by small ice crystals in three-dimensional space," *J. Opt. Soc. Amer. A*, vol. 13, no. 10, pp. 2072–2085, 1996.
[9] M. A. Yurkin and A. G. Hoekstra, "The discrete-dipole-approximation code ADDA: Capabilities and known limitations," *J. Quantitative Spectrosc. Radiative Transfer*, vol. 112, no. 13, pp. 2234–2247, Sep. 2011.
[10] R. F. Harrington, *Field Computation by Moment Methods*. New York, NY, USA: Wiley, 1993.
[11] M. L. Yang, Y. Q. Wu, X. Q. Sheng, and K. F. Ren, "Comparison of scattering diagrams of large nonspherical particles calculated by VCRM and MLFMA," *J. Quantitative Spectrosc. Radiative Transfer*, vol. 162, pp. 143–153, Sep. 2015.
[12] M. L. Yang, B. Y. Wu, H. W. Gao, and X. Q. Sheng, "A ternary parallelization approach of MLFMA for solving electromagnetic scattering problems with over 10 billion unknowns," *IEEE Trans. Antennas Propag.*, vol. 67, no. 11, pp. 6965–6978, Nov. 2019.
[13] H. Ling, R. C. Chou, and S. W. Lee, "Shooting and bouncing rays: Calculating the RCS of an arbitrarily shaped cavity," *IEEE Trans. Antennas Propag.*, vol. 37, no. 2, pp. 194–205, Feb. 1989.
[14] T. Q. Fan and L. X. Guo, "OpenGL-based hybrid GO/PO computation for RCS of electrically large complex objects," *IEEE Antennas Wireless Propag. Lett.*, vol. 13, pp. 666–669, 2014.
[15] C. L. Dong, L. X. Guo, X. Meng, and Y. Wang, "An accelerated SBR for EM scattering from the electrically large complex objects," *IEEE Antennas Wireless Propag. Lett.*, vol. 17, no. 12, pp. 2294–2298, Dec. 2018.
[16] W. F. Huang, Z. Q. Zhao, R. Zhao, J. Y. Wang, Z. P. Nie, and Q. H. Liu, "GO/PO and PTD with virtual divergence factor for fast analysis of scattering from concave complex targets," *IEEE Trans. Antennas Propag.*, vol. 63, no. 5, pp. 2170–2179, May 2015.
[17] K. F. Ren, F. Onofri, C. Rozé, and T. Girasole, "Vectorial complex ray model and application to two-dimensional scattering of plane wave by a spheroidal particle," *Opt. Lett.*, vol. 36, no. 3, pp. 370–372, 2011.
[18] K. F. Ren and C. Rozé, "Vectorial complex ray model for light scattering of nonspherical particles," in *Advances in Optics: Reviews*. Barcelona, Spain: Int. Frequency Sensor Assoc. Publishing, ch. 7, 2018, pp. 203–232.
[19] F. R. Onofri, K. F. Ren, M. Sentis, Q. Gaubert, and C. Pelcé, "Experimental validation of the vectorial complex ray model on the inter-caustics scattering of oblate droplets," *Opt. Exp.*, vol. 23, pp 15768–15773, 2015.
[20] Q. W. Duan, F. R. A. Onofri, X. E. Han, and K. F. Ren, "Generalized rainbow patterns of oblate drops simulated by a ray model in three dimensions," *Opt. Lett.*, vol. 46, pp. 4585–4588, 2021.
[21] K. Jiang, X. Han, and K. F. Ren, "Scattering from an elliptical cylinder by using the vectorial complex ray model," *Appl. Opt.*, vol. 51, no. 34, pp 8159–8167, 2012.
[22] C. Zhang, "Light scattering in the rainbow region of a large particle by vectorial complex ray model and physical optics," Ph.D. dissertation, Normandy University, Caen Cedex, France, Oct. 2022.
[23] K. F. Ren, "Software for the scattering of an elliptical particle by VCRM in a symmetric plane." Accessed: Mar. 5, 2014. [Online]. Available: https://amocops.univ-rouen.fr/en/content/download
[24] G. B. Airy, "On the intensity of light in the neighbourhood of a caustic," *Trans. Cambridge Philos. Soc.*, vol. 6, pp. 379–402, 1838.
[25] C. Zhang, C. Rozé, and K. F. Ren, "Airy theory revisited with the method combining vectorial complex ray model and physical optics," *Opt. Lett.*, vol. 47, no. 9, pp. 2149–2152, 2022.
[26] V. Khare and H. Nussenzveig, "Theory of the rainbow," *Phys. Rev. Lett.*, vol. 33, no. 16, pp. 976–980, Oct. 1974.
[27] G. P. Können and J. H. de Boer, "Polarized rainbow," *Appl. Opt.*, vol. 18, no. 12, pp 1961–1965, 1979.